

Three-dimensional structure of magnetic reconnection in a laboratory plasma

C. D. Cothran, M. Landreman, and M. R. Brown

Department of Physics and Astronomy, Swarthmore College, Swarthmore, Pennsylvania, USA

W. H. Matthaeus

Bartol Research Institute, University of Delaware, Newark, Delaware, USA

Received 22 October 2002; accepted 6 January 2003; published 6 March 2003.

[1] The local three-dimensional structure of magnetic reconnection has been measured for the first time in a magnetohydrodynamic (MHD) laboratory plasma at the Swarthmore Spheromak Experiment. An array of 600 magnetic probes which resolve ion inertial length and MHD time scale dynamics on a single shot basis measured the magnetic structure of partial spheromak merging events. Counter-helicity spheromaks merge rapidly, and reconnection activity clearly self-generates a local component of \mathbf{B} which breaks the standard 2D symmetry at the ion inertial scale. Consistent with prior results, no reconnection is observed for co-helicity merging. *INDEX TERMS:* 7835 Space Plasma Physics: Magnetic reconnection; 7831 Space Plasma Physics: Laboratory studies; 0649 Electromagnetics: Optics; *KEYWORDS:* magnetic reconnection, magnetohydrodynamics, plasma, laboratory, spheromak, ssx. *Citation:* Cothran, C. D., M. Landreman, M. R. Brown, and W. H. Matthaeus, Three-dimensional structure of magnetic reconnection in a laboratory plasma, *Geophys. Res. Lett.*, 30(5), 1213, doi:10.1029/2002GL016497, 2003.

1. Introduction

[2] Magnetic reconnection is a central feature of low frequency plasma dynamics in astrophysical and laboratory plasmas [Parker, 1979; Priest and Forbes, 2000]. Reconnection mediates the interaction of the solar wind and the magnetosphere at the terrestrial magnetopause [Sonnerup *et al.*, 1981; Øieroset *et al.*, 2001; Mozer *et al.*, 2002], and is an important dynamical feature in the magnetotail [Nagai *et al.*, 2001] and in planetary magnetospheres [Russell, 2002]. In the solar context, reconnection is a key feature of solar flare dynamics [Parker, 1957], and seems to be required to generate chromospheric fluctuations that heat the solar atmosphere [Axford and McKenzie, 1997]. In dynamo theory, reconnection transfers flux generated at small scales into large scale structures [Parker, 1979].

[3] Reconnection occurs when two bodies of highly conductive plasma bearing oppositely directed, embedded magnetic fields merge [Brown, 1999]. High conductivity implies that the magnetic field and fluid (plasma) motions are coupled. This condition fails in the reconnection layer where the inflow stagnates and the two bodies of magneto-fluid merge. Field lines convected into this region break and reconnect across the layer, producing a global change in the field topology. Magnetic energy consumed in the reconnection

layer is converted to heat, outflow kinetic energy, and individual particle acceleration.

[4] By assuming that the magnetic field and flows are everywhere coplanar, including within the reconnection region, a purely two-dimensional (2D) picture of reconnection is formed. Reconnection subject to this simplification has been studied theoretically [Parker, 1957; Petschek, 1964] and computationally [Matthaeus and Montgomery, 1981] for decades. A number of experimental studies deliberately enforce symmetries that facilitate interpretation [Stenzel and Gekelman, 1979; Ono *et al.*, 1993; Yamada *et al.*, 1997]. On all three fronts, theoretical, numerical, and experimental, attention has focused on planar X , Y , and O shaped magnetic structures [Brown, 1999; Yamada *et al.*, 1997; Stenzel and Gekelman, 1981]. While these efforts have yielded important insights, it is likely that the fundamental physics responsible for reconnection will not obey 2D restrictions. Furthermore, reconnection is free to take advantage of all three dimensions (3D) in any of its natural astrophysical instances. Recently, theoretical and numerical investigations have begun to explore collisionless reconnection in 2 1/2D [Mandt *et al.*, 1994; Shay *et al.*, 1998], with the notable consensus [Ma and Bhattacharjee, 2001; Shay *et al.*, 2001] that a vertical quadrupole field structure grows nonlinearly at the ion inertial scale due to the Hall effect [Biskamp *et al.*, 1995, 1997; Shay and Drake, 1998; Shay *et al.*, 1999; Bhattacharjee *et al.*, 2001].

[5] There have also been some experiments focused on 3D properties of reconnection. Compact toroid (CT) merging studies with the TS-3 [Ono *et al.*, 1997, 1996, 1993, 1990] machine measured co- and counter-helicity reconnection rate differences and observed ion heating by the “slingshot” effect, both of which are essentially 3D effects of the global toroidal geometry. However, 2D probe arrays were used for these magnetic structure measurements, and the geometry was made axisymmetric by construction. This enabled the poloidal flux function to be computed, thus inferring an axisymmetric reconnection rate. Reconnection and current sheet studies with the LAPD machine [Stenzel and Gekelman, 1979] used a linear 2D geometry. While 3D magnetic structure measurements were made by averaging over thousands of shots with a single movable probe in a highly reproducible plasma, the plasma was not in the MHD regime ($\rho_i \gg L$) and externally imposed vacuum fields were significant.

[6] In this Letter, we report the first experimental investigation of the 3D magnetic structure of reconnection in an MHD laboratory plasma. We present two main results, one

related to topology, the other to dynamics. First, we have clear evidence for the spontaneous generation of a component of the magnetic field \mathbf{B} normal to the conventional 2D X -structure. This fundamentally 3D feature [Hesse and Schindler, 1988] appears in the reconnection layer at the ion inertial scale, and may represent an asymmetric signature of the Hall effect. Second, we derive from the probe array data the first experimental visualization of the 3D merger of flux tubes at MHD scales. We note that the large scale dynamics in 3D is consistent with what others have observed in 2D, *vis.* flux tubes of opposite magnetic helicity (counter-helicity) merge much more readily than do flux tubes of the same helicity (co-helicity) [Ono *et al.*, 1990].

2. Experiment

[7] The magnetic structure measurements presented in this Letter were performed at the Swarthmore Spheromak Experiment (SSX) [Brown, 1999; Brown *et al.*, 2002a, 2002b] using a $5 \times 5 \times 8$ 3D array of vector magnetic probes inserted into a well defined volume where two spheromaks partially merge [Kornack *et al.*, 1998], as illustrated in Figure 1. Independent plasma guns at each end of SSX generate spheromaks [Geddes *et al.*, 1998] with either right-handed or left-handed magnetic helicity (twist). Figure 1 shows data for counter-helicity spheromaks. Two cylindrical copper flux conservers, 0.5 m in diameter, contain each spheromak. As indicated in the highlighted areas of the sketches in Figure 1, large back-to-back slots are cut out of the midplane walls of each flux conserver. The spheromaks therefore act as two reservoirs of magnetofluid which merge through the slots. Unique to SSX, this location is remote from the plasma sources (the guns): while neutral gas (hydrogen) and vacuum magnetic fields are introduced in the guns, only fully ionized plasma and embedded magnetic fields convect into the slots. The linear dimensions of the slots are large enough to allow significant interaction about the spheromak minor radius $a = 0.13$ m. Although the spheromaks are axisymmetric, the volume in the slots where the spheromaks merge (and where reconnection occurs) is inherently 3D. During the observed reconnection, the system is not externally driven, although it is never in complete equilibrium.

[8] The magnetic probe array measures the 3D magnetic structure formed when the spheromaks merge. Starting when the plasma guns fire ($t \equiv 0 \mu\text{s}$), the 200 measurements of \mathbf{B} are recorded every $0.8 \mu\text{s}$ for the lifetime of the spheromaks ($\approx 100 \mu\text{s}$) using a custom set of multiplexing electronics [Landreman *et al.*, 2003]. Detailed calibration and analysis of the probe array response with known test fields [Landreman *et al.*, 2003] indicate that the field measurements are accurate to an absolute error of approximately 20 G. The expanded views in Figure 1 show a sample of the data at $t = 64 \mu\text{s}$ from a single counter-helicity shot of SSX. Referring to the coordinate system introduced in Figure 1, the spatial resolution of the array is 1.5 cm in x and 1.9 cm in y and z . The magnetofluid inflow is along the $\pm\hat{z}$ directions into the slots.

[9] A variety of diagnostics have been used to characterize the SSX spheromaks. The plasma density, measured using quadrature laser interferometry to be $n_e \approx 5 \times 10^{13} \text{cm}^{-3}$, corresponds to an ion inertial scale of $c/\omega_{pi} \approx 2-3$ cm. Triple

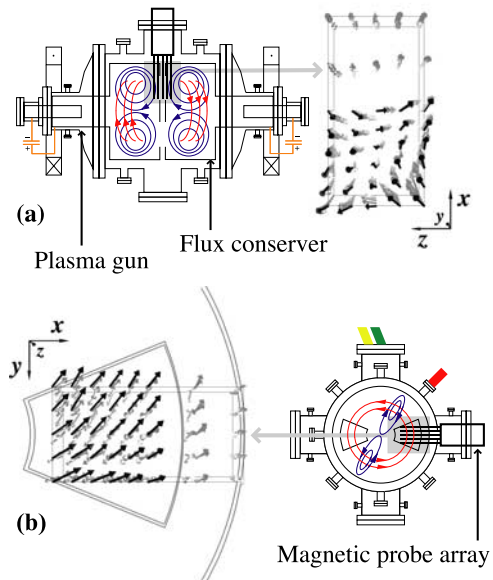


Figure 1. Top and end views of the Swarthmore Spheromak Experiment. Spheromaks generated by plasma guns partially merge across large slots cut in the midplane walls of the flux conservers. Magnetofluid flows into the slots in the $\pm\hat{z}$ direction. A magnetic probe array resolves the magnetic structure of the reconnection region at ion inertial length (2 cm) and MHD time ($0.8 \mu\text{s} < \tau_A$) scales. Magnified views show vector data for each of the 200 probe locations at $t = 64 \mu\text{s}$ after the plasma guns fired a counter-helicity shot. For clarity, only the facing planes of data in the views of (a) and (b) are highlighted. The largest fields shown are approximately 800 G.

Langmuir probes measure the electron temperature to be $T_e \approx 10-30$ eV, and energy analyzers estimate the ion temperature to be $T_i \approx 30$ eV. With an average magnetic field of ≈ 500 G, the ion gyroradius $\rho_I \approx 1$ cm is much smaller than the physical scale L of both the flux conservers and the region of interest near the slots, $\rho_I \ll L$. The Lundquist number S , the ratio of the resistive magnetic diffusion time $\tau_D = \mu_0 L^2 / \eta$ to the Alfvén transit time τ_A , is large for SSX, $S \approx 100-1000$. Accordingly, the SSX spheromaks are fully in the MHD regime ($S \gg 1$, $\rho_I \ll L$), and the resolution of the probe array measurements are at or below the characteristic MHD time and space scales.

3. Results

[10] Figure 2a summarizes the key topological result, obtained by integrating field lines and ribbons (sheets of field lines to accentuate the local twist) through the magnetic probe data of Figure 1. The four field ribbons drawn through the inflow (green) and outflow (gray) regions are seen to lie on a mostly planar 2D surface, indicating a magnetic structure consistent with the conventional paradigm for reconnection. These lines skirt the outer part of the reconnection region, staying a few c/ω_{pi} away from the center of the X -structure. However, the structure of the inner part of the reconnection region departs dramatically from any 2D expectations, as indicated by the fifth field ribbon

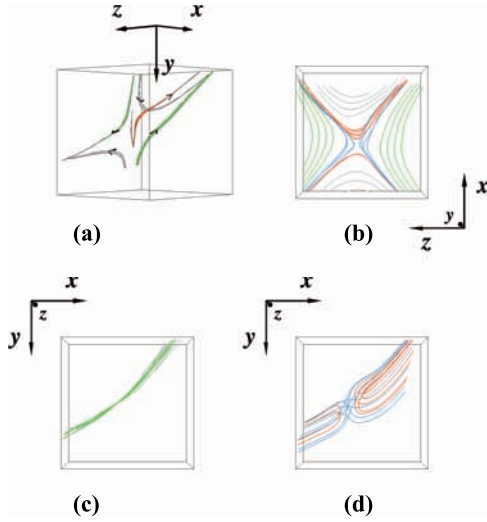


Figure 2. The 3D reconnection topology visualized with field lines and ribbons integrated through the data from Figure 1. (a) A self-generated guide field in the core of the reconnection region sweeps the red reconnected ribbon vertically ($\mathbf{E} \cdot \mathbf{B} > 0$). This purely 3D feature breaks the 2D symmetry seen a few c/ω_{pi} from the core, where green (inflow) and gray (outflow) ribbons trace a conventional 2D X structure. (b) The \hat{y} projection with more lines (blue/red are core lines with inflow/outflow connectivity). (c) The \hat{z} projection shows that lines through the outer reconnection region are coplanar. (d) The \hat{z} projection shows that lines through the inner (core) reconnection region are twisted into a 3D swept/sheared structure.

(red) of Figure 2a. This reconnected ribbon sweeps through the X -structure from below, indicating the 3D structure of the central part of the reconnection region.

[11] The remaining parts of Figure 2 expand upon this dual field structure. Figure 2b shows the \hat{y} projection of a set of field lines drawn through both the inner (blue/red) and outer (green/gray) parts of the reconnection region. The 2D behavior of the outer reconnection region is clearly seen in the \hat{z} projection of Figure 2c. In contrast, Figure 2d indicates the structure of the inner reconnection region. Both the reconnected (red) and unreconnected (blue) lines are swept and sheared normal to the X -structure. This behavior indicates the presence of a self-generated guide field normal to the X -structure and local to the core of the reconnection region. The magnitude of the normal field component in this region is 80 G for this shot, which is significantly greater than the systematic 20 G measurement error, and is about 10% of the inflow field strength.

[12] A heuristically appealing (though formally imprecise) definition of reconnection is the change of connectivity of magnetic flux tubes [Hesse and Schindler, 1988]. In Figure 3, this definition is applied to obtain the central dynamical result of this Letter. In Figure 3a and 3b, magnetic flux tubes are shown at two times from the same counter-helicity discharge as Figure 1. There is a clear suggestion that initially distinct flux tubes undergo merging by breaking and exchange of field lines. Initially private field lines ($t = 32 \mu\text{s}$) cross over, and experience a substantial degree of merger by $t = 64 \mu\text{s}$, corresponding to an estimated merging velocity of a few 10^5

cm/s. This represents a normalized reconnection rate of approximately $0.1 v_A$.

[13] In Figure 3c and 3d, similar flux tubes are shown for another discharge in which the current in one spheromak is reversed to study co-helicity interaction (both right-handed). Although the time interval is the same as in Figure 3a and 3b, here we see a much slower evolution. There is little or no suggestion of merging. Instead the flux tubes bend around one another while remaining distinct. This is similar to twisting of flux tubes reported for higher frequency electron MHD with unmagnetized ions [Gekelman and Pfister, 1988]. These 3D results are also consistent with previous 2D observations, namely that flux tubes of opposite magnetic helicity merge much more readily than do flux tubes of the same helicity [Ono *et al.*, 1990].

4. Discussion

[14] The origin of the self-generated field component indicated in Figure 2 is not clear. One outstanding possibility is that the Hall effect distorts the magnetic field within an ion inertial scale of the reconnection region. This is expected on the basis of both analytical and simulation studies [Shay *et al.*, 1998; Wang *et al.*, 2000]. In addition, there is some indication of the Hall effect on the structure of reconnection at the dayside magnetopause as measured by single spacecraft observations [Øieroset *et al.*, 2001; Mozer *et al.*, 2002]. However, the present results do not detect the characteristic Hall effect quadrupole structure, possibly due to the nonsteady and asymmetric nature of this “reconnec-

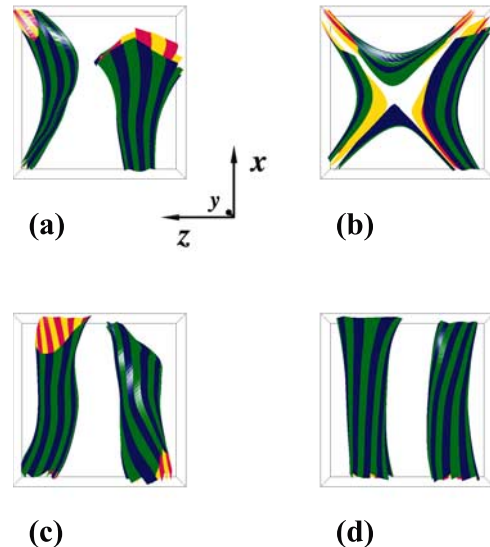


Figure 3. Interaction of magnetic flux tubes and helicity dependence. View along \hat{y} . Counter-helicity interaction (same data as Figure 1): (a) At $t = 32 \mu\text{s}$, flux is privately located on each side. (b) At $t = 64 \mu\text{s}$ (~ 10 Alfvén times later), flux has reconnected and formed a new flux bundle. Co-helicity interaction: (c) At $t = 32 \mu\text{s}$, flux is privately located as in (a) above. (d) At $t = 64 \mu\text{s}$, flux tubes wrap around one another but remain separate.

tion event.” We also cannot rule out limitations of the spatial probe resolution. Regardless of its origin, however, the self-generated field component indicates that 3D reconnection is occurring locally. Assuming that the reconnection electric field (not directly measured, but inferred from $-\mathbf{v} \times \mathbf{B}$ in the inflow regions) threads this region, we are observing an effect fundamentally associated with 3D “finite B” reconnection [Schindler *et al.*, 1988; Hesse and Schindler, 1988], namely a finite parallel electric field at the separator ($\mathbf{E} \cdot \mathbf{B} \neq 0$). This effect distinguishes 2D and 3D reconnection since $\mathbf{E} \cdot \mathbf{B} \equiv 0$ trivially for the classical 2D paradigm. Note that $\mathbf{E} \cdot \mathbf{B} > 0$ for the reconnected field line swept normal to the X-structure in Figure 2a.

5. Conclusion

[15] These first experimental results on the local 3D magnetic structure of MHD scale reconnection show some similarity to the expectations of 2D steady models, but also features that are intrinsically 3D. Familiar features include the expected 2D X-structure centered around a reconnection region, towards which magnetic flux is transported and from which emerge newly connected fields. Most importantly we describe fully 3D field effects: at the ion inertial scale, the reconnection region is nonsymmetric, nonsteady, and exhibits a characteristic swept/sheared structure. There is an apparent self-generation of a vertical guide field, resulting in “finite B” reconnection [Hesse and Schindler, 1988]. Flux tubes rendered from counter-helicity 3D data rapidly change from private unreconnected configurations into merged reconnected configurations, and the time scale for this appears to be compatible with fast reconnection at substantial fraction of the Alfvén speed.

[16] **Acknowledgments.** This work was performed under Department of Energy (DOE) grants DE-FG02-97ER54422 and DE-FG02-98ER54490. Discussions with P. Bellan of Caltech, and V. S. Lukin and T. Kornack of PPPL are gratefully acknowledged.

References

Axford, W. I., and J. F. McKenzie, in *The Solar Wind*, p. 31, Arizona Univ. Press, Tucson, 1997.

Bhattacharjee, A., et al., Recent developments in collisionless reconnection theory: Applications to laboratory and space plasmas, *Phys. Plasmas*, **8**, 1829, 2001.

Biskamp, D., et al., Ion controlled collisionless magnetic reconnection, *Phys. Rev. Lett.*, **75**, 3850, 1995.

Biskamp, D., et al., Two-fluid theory of collisionless magnetic reconnection, *Phys. Plasmas*, **4**, 1002, 1997.

Brown, M. R., Experimental studies of magnetic reconnection, *Phys. Plasmas*, **6**, 1717, 1999.

Brown, M. R., C. D. Cothran, et al., Experimental observation of energetic ions accelerated by three-dimensional magnetic reconnection in a laboratory plasma, *Astrophys. J.*, **577**, L63, 2002a.

Brown, M. R., C. D. Cothran, et al., Energetic particles from three-dimensional magnetic reconnection events in the swarthmore spheromak experiment, *Phys. Plasmas*, **9**, 2077, 2002b.

Geddes, C. G. R., T. W. Kornack, and M. R. Brown, Scaling studies of spheromak formation and equilibrium, *Phys. Plasmas*, **5**, 1027, 1998.

Gekelman, W., and H. Pfister, Experimental observations of the tearing of an electron current sheet, *Phys. Fluids*, **31**, 2017, 1988.

Hesse, M., and K. Schindler, A theoretical foundation of general magnetic reconnection, *J. Geophys. Res.*, **93**, 5559, 1988.

Kornack, T. W., P. K. Sollins, and M. R. Brown, Experimental observation of correlated magnetic reconnection and Alfvénic ion jets, *Phys. Rev. E*, **58**, R36, 1998.

Landreman, M., et al., Affordable and rapid multiplexed data acquisition: application to three-dimensional magnetic field measurements in a turbulent laboratory plasma, *Rev. Sci. Instrum.*, in press, 2003.

Ma, Z. W., and A. Bhattacharjee, Hall magnetohydrodynamic reconnection: The Geospace Environment Modeling challenge, *J. Geophys. Res.*, **106**, 3773, 2001.

Mandt, M. E., et al., Transition to whistler mediated magnetic reconnection, *Geophys. Res. Lett.*, **21**, 73, 1994.

Matthaeus, W. H., and D. Montgomery, Nonlinear evolution of the sheet pinch, *J. Plasma Phys.*, **25**, 11, 1981.

Mozer, F., S. D. Bale, and T. D. Phan, Evidence of diffusion regions at a subsolar magnetopause crossing, *Phys. Rev. Lett.*, **89**, 015,002, 2002.

Nagai, T., I. Shinohara, et al., Geotail observations of the hall current system: Evidence of magnetic reconnection in the magnetotail, *J. Geophys. Res.*, **106**, 25929, 2001.

Øieroset, M., et al., In situ detection of collisionless reconnection in the earth’s magnetotail, *Nature*, **412**, 414, 2001.

Ono, Y., et al., Magnetic reconnection of plasma toroids with cohericity and counterhelicity, *Phys. Rev. Lett.*, **65**, 721, 1990.

Ono, Y., et al., Experimental investigation of three-dimensional magnetic reconnection by use of two colliding spheromaks, *Phys. Fluids B*, **5**, 3691, 1993.

Ono, Y., et al., Ion acceleration and direct ion heating in three-component magnetic reconnection, *Phys. Rev. Lett.*, **76**, 3328, 1996.

Ono, Y., et al., Experimental investigation of three-component magnetic reconnection by use of merging spheromaks and tokamaks, *Phys. Plasmas*, **4**, 1953, 1997.

Parker, E. N., Sweet’s mechanism for merging magnetic fields in conducting fluids, *J. Geophys. Res.*, **62**, 509, 1957.

Parker, E. N., *Cosmical Magnetic Fields: Their Origin and Activity*, Oxford Univ. Press, New York, 1979.

Petschek, H. G., Magnetic annihilation, in *AAS-NASA Symposium on the Physics of Solar Flares*, edited by W. N. Hess, p. 425, *NASA Spec. Publ.*, **50**, 1964.

Priest, E. R., and T. G. Forbes, *Magnetic Reconnection*, Cambridge Univ. Press, New York, 2000.

Russell, C. T., Reconnection in planetary magnetospheres, *Adv. Space Res.*, **29**, 1045, 2002.

Schindler, K., et al., General magnetic reconnection, parallel electric fields and helicity, *J. Geophys. Res.*, **93**, 5547, 1988.

Shay, M. A., and J. F. Drake, The role of electron dissipation on the rate of collisionless magnetic reconnection, *Geophys. Res. Lett.*, **25**, 3759, 1998.

Shay, M. A., et al., Structure of the dissipation region during collisionless magnetic reconnection, *J. Geophys. Res.*, **103**, 9165, 1998.

Shay, M. A., et al., The scaling of collisionless magnetic reconnection for large systems, *Geophys. Res. Lett.*, **26**, 2163, 1999.

Shay, M. A., et al., Alfvénic collisionless magnetic reconnection and the hall term, *J. Geophys. Res.*, **106**, 3759, 2001.

Sonnerup, B. U. O., et al., Evidence for magnetic field reconnection at the Earth’s magnetopause, *J. Geophys. Res.*, **86**, 10049, 1981.

Stenzel, R. L., and W. Gekelman, Experiments on magnetic field line reconnection, *Phys. Rev. Lett.*, **42**, 1055, 1979.

Stenzel, R. L., and W. Gekelman, Magnetic field line reconnection experiments, 1, Field topologies, *J. Geophys. Res.*, **86**, 649, 1981.

Wang, X., A. Bhattacharjee, and Z. W. Ma, Collisionless reconnection: Effects of hall current and electron pressure gradient, *J. Geophys. Res.*, **105**, 27633, 2000.

Yamada, M., et al., Identification of Y-shaped and O-shaped diffusion regions during magnetic reconnection in a laboratory plasma, *Phys. Rev. Lett.*, **78**, 3117, 1997.

M. R. Brown, C. D. Cothran, and M. Landreman, Department of Physics and Astronomy, Swarthmore College, Swarthmore, PA 19081, USA. (ccothral@swarthmore.edu)

W. H. Matthaeus, Bartol Research Institute, University of Delaware, Newark, DE 19716, USA.